General Disclaimer

One or more of the Following Statements may affect this Document

- This document has been reproduced from the best copy furnished by the organizational source. It is being released in the interest of making available as much information as possible.

- This document may contain data, which exceeds the sheet parameters. It was furnished in this condition by the organizational source and is the best copy available.

- This document may contain tone-on-tone or color graphs, charts and/or pictures, which have been reproduced in black and white.

- This document is paginated as submitted by the original source.

- Portions of this document are not fully legible due to the historical nature of some of the material. However, it is the best reproduction available from the original submission.

Produced by the NASA Center for Aerospace Information (CASI)

BM52/Lettie Reed

NATIONAL AERONAUTICS AND SPACE ADMINISTRATION

NASA General Working Paper No. 10,084

A DESIGN PARAMETER SYNTHESIS DERIVED FROM A MATHEMATICAL ANALYSIS OF A HYPOTHETICAL LUNAR FLYING VEHICLE

N70-34395
(ACCESSION NUMBER)
35
(PAGES)
TMX-64333
(NASA CR OR TMX OR AD NUMBER)
(THRU)
1
(CODE)
31
(CATEGORY)
FACILITY FORM 602

AUG 1970
RECEIVED
NASA STI FACILITY
INPUT BRANCH

[redacted]

MANNED SPACECRAFT CENTER
HOUSTON, TEXAS
April 11, 1969

NASA GENERAL WORKING PAPER NO. 10,084

A DESIGN PARAMETER SYNTHESIS DERIVED FROM A MATHEMATICAL ANALYSIS OF A HYPOTHETICAL LUNAR FLYING VEHICLE

PREPARED BY

for William M. Jacqmein
Flight Technology Branch

David L. Hall
Flight Technology Branch

for Mark K. Craig
Flight Technology Branch

AUTHORIZED FOR DISTRIBUTION

for Maxime A. Faget
Director of Engineering and Development

NATIONAL AERONAUTICS AND SPACE ADMINISTRATION
MANNED SPACECRAFT CENTER
HOUSTON, TEXAS
April 11, 1969

PRECEDING PAGE BLANK NOT FILMED.

CONTENTS

Section	Page
SUMMARY	1
INTRODUCTION	1
SYMBOLS	2
SYSTEM PARAMETER ANALYSIS	5
Discussion of Equations	5
Human-Pilot Describing Function	9
Development of Graphs	10
SYSTEM CONFIGURATION ANALYSIS	11
RESULTS	16
Stability Maps	16
Stable-Area Dependence Upon Pilot-Describing Parameters	18
Nyquist Plots	18
CONCLUSIONS	19
REFERENCES	20
BIBLIOGRAPHY	20

FIGURES

Figure		Page
1	Vehicle coordinate system for kinesthetic- and thrust-vector control	21
2	Hurwitz-minor zero lines	22
3	Stability interpretation of Hurwitz-minor zero lines	23
4	Stable-region definition in the A_{i1}-A_{i2} plane	24
5	Stability limit for comfortable human-parameter values in the A_{i1}-A_{i2} plane	25
6	System-stability dependence upon pilot gain as exhibited by Nyquist plots	26
7	Ratio M of output to input as a function of vehicle parameters A_{i1} and A_{i2}	27
8	Comparison of A_{i1}-A_{i2} stable regions as determined by the ratio M of output to input and the Hurwitz-minor zero line	28
9	Spring constant as a function of damping coefficient for various stable vehicle configurations	29
10	Vehicle configuration with one mass above and the other mass below the gimbal point	30
11	Favorable vehicle configurations	
	(a) Thrust-vector control	31
	(b) Kinesthetic vehicle control	32

A DESIGN PARAMETER SYNTHESIS DERIVED FROM A MATHEMATICAL ANALYSIS OF A HYPOTHETICAL LUNAR FLYING VEHICLE

By William A. Jacqmein, David L. Hall, and Mark K. Craig

SUMMARY

The purpose of this study is to develop design information from a mathematical analysis of a manually controlled lunar flying vehicle found in NASA General Working Paper No. 10,079 (ref. 1). The equations developed in that paper are discussed with respect to feasible vehicle configurations and the corresponding differences which arise from the use of thrust-vector as opposed to kinesthetic control. Experimental data concerning the human-pilot describing function are employed in the development of a stable region and a region of comfortable control expressed in terms of vehicle parameters. The equations representing vehicle parameters are investigated, and favorable lunar flying vehicle configurations indicated by this analysis are described.

INTRODUCTION

This paper is a study of the equations developed in the paper "A Mathematical Analysis of the Stability of a Lunar Flying Vehicle with Manual Controls." In that paper, the vehicle equations of motion were developed using the Lagrange energy equation and were subsequently solved for the angular accelerations. The equations were then transformed to the state-variable matrix notation by use of the Jacobian. Vehicle control was represented by the experimentally determined pilot describing function. The vehicle-control and -dynamics equations were combined; the closed-loop system characteristic equation was then derived and represented in Hurwitz matrix form yielding the principal minors. This study analyzes both the system characteristic equation and the system open-loop transfer function by means of various algebraic and geometric stability criteria to derive design-related vehicle parameter information.

SYMBOLS

A_{ij}	vehicle parameter term
c	damping coefficient
D	dissipation function
$\frac{d(\ )}{dq}$	derivative of ( ) with respect to q
F_c	control force
$G(\ )$	open-loop transfer function
g	gravity
H_n	Hurwitz-matrix principal minor
I	moment of inertia
j	$\sqrt{-1}$
K_p	pilot gain
k	spring constant
L_1	directed length from mass-1 center of gravity to gimbal point
L_2	directed length from gimbal to mass-2 center of gravity
L_c	directed length from gimbal to application of control force
M	ratio of output to input
M_n	mass
Q_n	general force term
q_n	generalized coordinate
r_o	radius of circle

T engine thrust

T_e kinetic energy function

T_I general lag-time constant

T_L general lead-time constant

T_N first-order neuromuscular system lag-time-constant approximation

T_{N_1} first-order neuromuscular system lag-time constant

t time

V potential energy function

X_n coordinate of mass n center of gravity

x_b body axis

Y_c control-element transfer function

Y_p pilot describing function

Z_n coordinate of mass n center of gravity

z_b body axis

α,α' constant term in A_{ij} vehicle parameter

β coordinate of mass-2 angular position

δ gimbal angle

Δ matrix determinant

ζ_N damping ratio of the second-order component of the neuromuscular system

θ coordinate of mass-1 angular position

λ, λ' constant term in A_{i1} vehicle parameter

τ pilot reaction time lag

ψ $\sin^{-1}(\frac{1}{M})$

ω general frequency

ω_N undamped natural frequency of the second-order component of the neuromuscular system

$\frac{\partial(\ )}{\partial q}$ partial derivative of ( ) with respect to q

Subscripts:

1 mass 1

2 mass 2

b body

c control

i matrix row designation

j matrix column designation

N neuromuscular system

n integer

p pilot

Operators:

$(\dot{\ })$ first derivative of ( ) with respect to time

$(\ddot{\ })$ second derivative of ( ) with respect to time

s Laplace transformation operator

SYSTEM PARAMETER ANALYSIS

Discussion of Equations

The rotational stability characteristics of the proposed manually controlled lunar flying vehicle are described by the equation (ref. 1)

$$\begin{aligned}\frac{\tau}{2} T_I T_N s^5 &+ \left[\frac{\tau}{2}\left(T_I + T_N\right) + T_I T_N\right] s^4 \\ &+ \left[\frac{\tau}{2}\left(1 - K_p A_{22} T_L\right) + T_I + T_N\right] s^3 \\ &+ \left\{1 + K_p\left[A_{22}\left(T_L - \frac{\tau}{2}\right) - \frac{\tau}{2} A_{21} T_L\right]\right\} s^2 \\ &+ K_p\left[A_{22} + A_{21}\left(T_L - \frac{\tau}{2}\right)\right] s + K_p A_{21} = 0 \end{aligned} \tag{1}$$

The formulation of this equation using vehicle parameter terms A_{21} and A_{22} represents a two-mass system manually controlled by thrust-vector manipulation about a gimbal point. The vehicle is considered to be mass 1 and the engine, mass 2 (fig. 1). If, on the other hand, the vehicle is considered to be kinesthetically controlled, the vehicle is designated as mass 2 and the pilot as mass 1. As a consequence, the pitch angle, which was θ in the first case, becomes β in the second case. The equation defining the rotational stability characteristics for this kinesthetically controlled vehicle can be found by examining the matrix describing vehicle rotational motion (ref. 1).

$$\begin{bmatrix} \dot{\theta} \\ \ddot{\theta} \\ \dot{\beta} \\ \ddot{\beta} \end{bmatrix} = \begin{bmatrix} 0 & 1 & 0 & 0 \\ A_{21} & A_{22} & A_{23} & A_{24} \\ 0 & 0 & 0 & 1 \\ A_{41} & A_{42} & A_{43} & A_{44} \end{bmatrix} \begin{bmatrix} \theta \\ \dot{\theta} \\ \beta \\ \dot{\beta} \end{bmatrix} + \begin{bmatrix} 0 \\ A_{25} \\ 0 \\ A_{45} \end{bmatrix} F_c \tag{2}$$

When the fourth line is rewritten in terms of the gimbal angle δ, the representation of the pitch angle becomes

$$\ddot{\beta} = A_{41}\delta + A_{42}\dot{\delta} \tag{3}$$

Performing a Laplace transformation and rearranging terms yields the transfer function for the dynamics of a kinesthetically controlled vehicle

$$Y_c = \frac{\beta}{\delta} = \frac{A_{42}s + A_{41}}{s^2} \tag{4}$$

The transfer function for the dynamics of a thrust-vector-controlled vehicle, obtained through a similar procedure, is

$$Y_c = \frac{\theta}{\delta} = \frac{A_{22}s + A_{21}}{s^2} \tag{5}$$

The equation defining the rotational-stability characteristics of a kinesthetically controlled vehicle is, therefore, that of a thrust-vector-controlled vehicle (eq. (1)), with the exception that A_{21} is replaced by A_{41}, and A_{22} is replaced by A_{42}.

The A_{ij} terms represent vehicle parameters extracted from the state-variable matrix describing vehicle rotational motion. These parameters are (ref. 1)

$$A_{21} = -A_{23} = -\frac{1}{\Delta}\left\{k\left(M_1 + M_2\right)\left[\left(M_1 + M_2\right)I_2 + M_1M_2L_2\left(L_1 + L_2\right)\right] + M_1TL_1\left(M_1I_2 + M_1M_2L_2^{\,2} + M_2I_2\right)\right\} \tag{6}$$

$$A_{22} = -A_{24} = -\frac{1}{\Delta}c\left(M_1 + M_2\right)\left[\left(M_1 + M_2\right)I_2 + M_1M_2L_2\left(L_1 + L_2\right)\right] \tag{7}$$

$$A_{41} = -A_{43} = \frac{1}{\Delta}\left\{k\left(M_1 + M_2\right)\left[\left(M_1 + M_2\right)I_1 + M_1M_2L_1\left(L_1 + L_2\right)\right] + M_1{}^2M_2TL_1{}^2L_2\right\} \tag{8}$$

$$A_{42} = -A_{44} = \frac{1}{\Delta}\, c\left(M_1 + M_2\right)\left[\left(M_1 + M_2\right)I_1 + M_1M_2L_1\left(L_1 + L_2\right)\right] \tag{9}$$

$$\Delta = \left(M_1 + M_2\right)\left[I_2M_2\left(I_1 + M_1L_1{}^2\right) + I_1M_1\left(I_2 + M_2L_2{}^2\right)\right] \tag{10}$$

The Hurwitz algorithm determines the criteria which the system characteristic equation (eq. (1)) must satisfy so that stability can be attained. The necessary and sufficient condition for equation (1) to be a Hurwitz polynomial (and, thus, indicative of system stability) is that the principal minors of the Hurwitz matrix all be positive. The principal minors of the Hurwitz matrix, as found in reference 1, are

$$H_1 = \frac{\frac{\tau}{2}\left(T_I + T_N\right) + T_IT_N}{\frac{\tau}{2}\, T_IT_N} \tag{11}$$

$$\begin{aligned} H_2 = {} & \frac{\frac{\tau^2}{4}\left(T_I + T_N\right) + \frac{\tau}{2}\left(T_I{}^2 + T_N{}^2\right) + T_IT_N\left(T_I + T_N + \tau\right)}{\left(\frac{\tau}{2}\, T_IT_N\right)^2} \\ & + \frac{K_p}{\left(\frac{\tau}{2}\, T_IT_N\right)^2}\left\{A_{i2}\left[T_IT_N\left(\frac{\tau^2}{4} - \tau T_L\right) - \frac{\tau^2}{4}\left(T_I + T_N\right)T_L\right]\right. \\ & \left. + A_{i1}\frac{\tau^2}{4}\, T_IT_NT_L\right\} \end{aligned} \tag{12}$$

$$H_3 = \frac{H_2}{\frac{\tau}{2} T_I T_N} \left\{ 1 + K_p \left[A_{i2}\left(T_L - \frac{\tau}{2}\right) - A_{i1} \frac{\tau}{2} T_L \right] \right\}$$

$$+ \frac{\left[\frac{\tau}{2}\left(T_I + T_N\right) + T_I T_N\right]}{\left(\frac{\tau}{2} T_I T_N\right)^3} K_p \left\{ A_{i1} \left[T_I T_N (\tau - T_L) \right.\right.$$

$$\left.\left. + \frac{\tau}{2}\left(T_I + T_N\right)\left(\frac{\tau}{2} - T_L\right)\right] - A_{i2}\left[\frac{\tau}{2}\left(T_I + T_N\right) + T_I T_N\right] \right\} \qquad (13)$$

$$H_4 = \frac{K_p}{\left(\frac{\tau}{2} T_I T_N\right)^2} \left\{ H_3 \frac{\tau}{2} T_I T_N \left[A_{i2} + A_{i1}\left(T_L - \frac{\tau}{2}\right)\right] \right.$$

$$\left. - H_2 A_{i1} \left[\frac{\tau}{2}\left(1 - K_p A_{i2} T_L\right) + T_I + T_N \right] \right\}$$

$$+ \frac{K_p^{\,2} A_{i1}}{\left(\frac{\tau}{2} T_I T_N\right)^3} \left\{ A_{i2} \left[\frac{\tau}{2}\left(T_I + T_N\right) + T_I T_N \right] \right.$$

$$\left. + A_{i1} \left[\left(T_I + T_N\right)\left(T_L - \frac{\tau}{2}\right)\frac{\tau}{2} + T_I T_N \left(T_L - \tau\right) \right] \right\} \qquad (14)$$

$$H_5 = \frac{H_4 K_p A_{i1}}{\frac{\tau}{2} T_I T_N} \qquad (15)$$

Another method of evaluating system stability employs the open-loop transfer function

$$Y_c Y_p = \frac{K_p\left(T_L s + 1\right)\left(-\frac{\tau}{2} s + 1\right)\left(A_{i2} s + A_{i1}\right)}{s^2\left(T_I s + 1\right)\left(T_N s + 1\right)\left(\frac{\tau}{2} s + 1\right)} = G(s) \qquad (16)$$

Stability in this instance is determined by replacing s in $G(s)$ with $j\omega$ and plotting the function $G(j\omega)$ for an increasing ω. By the Nyquist criterion, the system is stable if the vector locus of $G(j\omega)$ drawn from $\omega = 0$ to $\omega \rightarrow +\infty$ (in the sense of increasing ω) encircles the point (-1,0) in a counterclockwise direction. If the system is found to be stable, its degree of stability can be approximated by constructing a circle with center on the negative real axis which is mutually tangent to the function $G(j\omega)$ and to a line from the origin at an angle ψ, where $\psi = \sin^{-1}(1/M)$. The degree of stability can be evaluated using the equation for the radius of the circle

$$r_o = \frac{M}{M^2 - 1} \tag{17}$$

An indication of the relative stability between two points can be gained by isolating the ratio of output to input M. An increasing M decreases the system stability. Acceptable stability requires that $1 < M \leq 1.4$ (ref. 2).

Human-Pilot Describing Function

The determination of the range of values assigned to the parameters of the human-pilot describing function is prerequisite to a numerical analysis of a man-vehicle system. The experimentally determined ranges of these parameters, as established by Skolnik (ref. 3), are the following:

Gain, K_p	0.6 to 250.0
Lead time, T_L	0.0 to 5.3
Lag time, T_I	0.0 to 25.0
Reaction time, τ	0.1 to 0.4
Neuromuscular lag time, T_N	0.1 to 0.7

It has been established by McRuer (ref. 4), however, that neuromuscular lag time has little effect upon the pilot describing function. Consistent with this, McRuer demonstrates that a lag time of 0.1 yields results of good accuracy.

Reaction time τ is influenced by the complexity of the task, as well as by such tenuous parameters as fatigue, vibration, display

system, et cetera. Single-axis control experiments concerning human-pilot describing functions generally utilize a reaction time of approximately 0.15.

Experimental evidence indicates that the pilot is more satisfied with the control characteristics of a system when certain conditions have been met. At present, no precise data exist on exactly what constitutes this comfortable control system with respect to parameter definition. Various experiments, however, have yielded useful general observations. The most satisfactory system appears to be one in which the pilot acts as a simple gain and does not utilize the equalization constant, lead-lag compensation. Experimental evidence indicates that the pilot prefers small values of lead, lag, and gain if this situation cannot be attained. Of these parameters, a small lead time appears to be the most decisive in the determination of what constitutes a comfortable control system. According to these general observations, a comfortable control region can be approximated by limiting the range values of the pilot parameters to the following:

Gain, K_p	0.6 to 5.0
Lead time, T_L	0.0 to 1.0
Lag time, T_I	0.0 to 5.0
Reaction time, τ	0.15
Neuromuscular lag time, T_N	0.10

Development of Graphs

Principal minors of the Hurwitz matrix (eqs. (11) to (15)) can be used to develop maps of stable regions in the A_{i1}-A_{i2} plane, by holding the human-parameter values constant while selecting an arbitrary value of A_{i1} and subsequently solving for the value of A_{i2}, which yields a minor value of zero. Trends established by all points generated in this manner (fig. 2) determine the boundary between the positive and negative values of the minor and, thus, by the Hurwitz criterion, designate the periphery of stability in the A_{i1}-A_{i2} plane. Stability is attained in a region where each of the Hurwitz minors has a positive value associated with its A_{i1}-A_{i2} coordinate location (fig. 3). The summation of each of the stable regions associated with a fixed set of human-parameter values over the entire spectrum of these values yields a stability map that is applicable to any given set of human parameters (fig. 4). A similar procedure is followed in

the development of a stability map for the special case of human-parameter values which are within the previously established comfortable region (fig. 5).

Redefinition and subsequent verification of these stability maps can be undertaken using the Nyquist criterion. Procedure dictates that the term s in the system open-loop transfer function $G(s)$ (eq. (16)) be replaced by $j\omega$ and that $G(j\omega)$ be plotted for an increasing ω, holding all other terms constant (fig. 6). The previously discussed extension of the Nyquist procedure (eq. (17)) provides a means of expressing the ratio of output to input M as a function of the A_{ij} vehicle parameters (fig. 7). In so doing, regions of stability defined by the ratio of output to input can be compared to those defined by the Hurwitz criterion (fig. 8).

A qualitative indication of the interaction between the system-damping coefficient c and the system-spring constant k is presented in figure 9 for the specific lunar flying vehicle configuration depicted in figure 10. The interaction was developed by estimating vehicle characteristics corresponding to the stability boundary in the A_{i1}-A_{i2} plane. Values of A_{i1} and A_{i2} were then calculated using these characteristics and were subsequently set equal to the A_{ij} values of the nearest point on the boundary of the stable region. The A_{ij} equations (eqs. (6) to (10)) were then solved for k and c. Points were selected along other portions of the stability boundary and the process was repeated. This procedure was followed for lunar flying vehicles (both kinesthetically and thrust-vector controlled) of various masses and inertias over the same range of A_{ij} values.

SYSTEM CONFIGURATION ANALYSIS

The state-variable-matrix equation describing vehicle rotational stability (eq. (2)) represents a gimbal-controlled two-mass lunar flying vehicle. Equation (2) imposes the constraint, however, that the centers of gravity of both masses be on the same side of the gimbal. Therefore, the applicability of this equation to cases in which the centers of gravity are on different sides of the gimbal point must be determined.

The state-variable matrix is derived from application of Lagrange's equation

$$Q_n = \frac{d}{dt}\left(\frac{\partial T_e}{\partial \dot{q}_n}\right) - \frac{\partial T_e}{\partial q_n} + \frac{\partial D}{\partial \dot{q}_n} + \frac{\partial V}{\partial q_n} \tag{18}$$

The kinetic energy function T_e is

$$\begin{aligned} T_e = {} & \frac{M_1}{2}\left(\dot{X}_1{}^2 + \dot{Z}_1{}^2\right) + \frac{I_1}{2}\dot{\theta}^2 \\ & + \frac{M_2}{2}\Big[\dot{X}_1{}^2 + \dot{Z}_1{}^2 + L_1{}^2\dot{\theta}^2 + L_2{}^2\dot{\beta}^2 \\ & + 2L_1\dot{\theta}\left(\dot{X}_1 \cos\theta - \dot{Z}_1 \sin\theta\right) \\ & + 2L_2\dot{\beta}\left(\dot{X}_1 \cos\beta - \dot{Z}_1 \sin\beta\right) \\ & + 2L_1L_2\dot{\theta}\dot{\beta}\cos(\theta - \beta)\Big] + \frac{I_2}{2}\dot{\beta}^2 \end{aligned} \tag{19}$$

The dissipation function for rotational motion between two bodies is

$$D = \frac{c}{2}(\dot{\theta} - \dot{\beta})^2 \tag{20}$$

The potential energy function is expressed by

$$V = M_1 g Z_1 + M_2 g\left(Z_1 + L_1 \cos\theta + L_2 \cos\beta\right) + \frac{k}{2}(\theta - \beta)^2 \tag{21}$$

Referring to the kinetic energy term T_e (eq. (19)), the equations describing the velocity of mass 2 in relation to mass 1 are

$$\dot{X}_2 = \dot{X}_1 + L_1\dot{\theta} \cos \theta + L_2\dot{\beta} \cos \beta \tag{22}$$

$$\dot{Z}_2 = \dot{Z}_1 - L_1\dot{\theta} \sin \theta - L_2\dot{\beta} \sin \beta \tag{23}$$

These are the critical relations in determining the applicability of the kinetic energy term to a configuration in which the center of gravity (c.g.) of one mass is above the gimbal point, and the c.g. of the other is below the gimbal point. In an arbitrary configuration (fig. 10), the vectors representing the motion of the gimbal point with respect to mass 1 and the motion of mass 2 with respect to the gimbal point are both negative in the X and Z directions. The second and third terms of $\dot{X}_2$ and $\dot{Z}_2$, therefore, should be negative. In figure 10, L_1, L_2, θ, and β are also negative. Substitution into equations (22) and (23) yields

$$\dot{X}_2 = \dot{X}_1 - L_1\dot{\theta} \cos \theta - L_2\dot{\beta} \cos \beta \tag{24}$$

$$\dot{Z}_2 = \dot{Z}_1 - L_1\dot{\theta} \sin \theta - L_2\dot{\beta} \sin \beta \tag{25}$$

Formulation of the relative-velocity equations from the configuration dynamics yields the same results. The relative-velocity equations (and hence, their conjugate kinetic energy term) are, therefore, independent of two-mass c.g. distribution about the gimbal point.

Investigation indicated that only the magnitude of the damping term D (eq. (20)) would be altered by the proposed configuration extension. Similarly, the potential energy relation V (eq. (21)) need be considered only to the extent that the point of zero potential energy must be redefined to occur when L_1 and L_2 are 180° apart.

The general force term Q_n of the Lagrange energy equation (eq. (18)) varies in form if the centers of gravity of the two masses are on different sides of the gimbal. Originally

$$Q_1 = - TL_1 \sin(\theta - \beta) \tag{26}$$

$$Q_2 = - F_c L_c \tag{27}$$

$$Q_3 = T \sin \beta + F_c \cos \theta \tag{28}$$

$$Q_4 = T \cos \beta - F_c \sin \theta \tag{29}$$

If, however, one center of gravity is above the gimbal point and the other below, the resulting Q_n terms are

$$Q_1 = - TL_1 \sin(\theta - \beta) \tag{30}$$

$$Q_2 = F_c L_c \tag{31}$$

$$Q_3 = T \sin \beta - F_c \cos \theta \tag{32}$$

$$Q_4 = T \cos \beta + F_c \sin \theta \tag{33}$$

Examination of the equations describing vehicle rotational motion (eq. (2)), however, reveals that the F_c term affects only the constant added to the matrix and, hence, does not influence the system-characteristic equation.

Thus, a term-by-term analysis of the Lagrange energy equation shows the system-characteristic equation to be independent of the distribution about the gimbal point of the centers of gravity of the two system masses. The characteristic equation can, therefore, be used without restriction to indicate preferable vehicle configurations.

Stability maps (fig. 4) generated by the Hurwitz criterion reveal that a necessary, but not sufficient, condition for the realization of vehicle stability is that parameter terms A_{i1} and A_{i2} have the same sign. Keeping this in mind, a useful generalization as to system preferability can be concluded from an examination of these A_{ij} terms (eqs. (6) to (10)). In simplified form they are

$$A_{21} = \pm\alpha k \pm \lambda \tag{34}$$

$$A_{22} = \pm\alpha c \tag{35}$$

$$A_{41} = \pm\alpha' k \pm \lambda \tag{36}$$

$$A_{42} = \pm\alpha' c \tag{37}$$

The factors which influence the sign associated with an A_{ij} quantity are the sign and relative magnitude of L_1 and L_2. The system spring constant k is neglected, because a system in which the pilot will not be called upon to input a spring-constant value is preferred. A preferable vehicle configuration, therefore, requires that the signs of α and λ be the same in order that the signs of A_{i1} and A_{i2} be the same (a stable system). Figure 10 is an example of an unpreferable system. Assuming this configuration to be kinesthetically controlled, the applicable vehicle parameter terms are A_{41} and A_{42}. Mass 1 is the center of gravity of the man; mass 2 is the center of gravity of the vehicle, and the gimbal point is the man's ankles. Considering L_1 to be greater than L_2, which is normally the case, results in a system similar to current kinesthetic control vehicle simulators. When L_1 and L_2 are substituted into equations (6) to (10), the resulting relations are

$$A_{41} = \alpha k - \lambda \tag{38}$$

$$A_{42} = \alpha c \tag{39}$$

Because the signs of α and λ are different, the pilot must input some spring-constant value to attain stability; consequently, the configuration is considered unpreferable. Figure 11 presents arrangements of centers of gravity and gimbal points which are considered preferable by the previously established criteria; some, of course, are physically unrealistic.

RESULTS

Stability Maps

Stability maps (fig. 2) describing the zero lines of the Hurwitz minors reveal, in accordance with theory, that minor H_4 is the determining minor. If H_4 is positive, each of the other minors is also positive. The zero line of minor H_4 always passes through the origin in the A_{i1}-A_{i2} plane. The stable region, therefore, does not transcend the abscissa and, thus, exists either entirely above or below the A_{i1} axis. Consistent with the positive minor stability criteria is the fact that the last term of the system-characteristic equation $K_p A_{i1}$ must be positive (K_p and A_{i1} must have the same sign). A negative $K_p A_{i1}$ creates a root with positive real part in the solution, which is indicative of divergent and, thus, unstable motion. Since A_{i1} and A_{i2} must have the same sign, the vehicle parameters must place A_{i1} and A_{i2} values in the first quadrant for stability to be attained, if the pilot adopts a positive gain. If the pilot inputs a negative gain, on the other hand, stability requires that vehicle parameters A_{i1} and A_{i2} be in the third quadrant. A vehicle whose A_{ij} parameters place it in the second or fourth quadrant will be unstable.

Minor H_4 is described by

$$H_4 = \frac{K_p}{\left(\frac{\tau}{2} T_I T_N\right)^2} \left\{ H_3 \frac{\tau}{2} T_I T_N \left[A_{i2} + A_{i1}\left(T_L - \frac{\tau}{2}\right)\right] \right.$$

$$\left. - H_2 A_{i1} \left[\frac{\tau}{2}\left(1 - K_p A_{i2} T_L\right) + T_I + T_N \right] \right\}$$

$$+ \frac{K_p^{\,2} A_{i1}}{\left(\frac{\tau}{2} T_I T_N\right)^3} \left\{ A_{i2} \left[\frac{\tau}{2}\left(T_I + T_N\right) + T_I T_N \right] \right.$$

$$\left. + A_{i1}\left[\left(T_I + T_N\right)\left(T_L - \frac{\tau}{2}\right)\frac{\tau}{2} + T_I T_N\left(T_L - \tau\right)\right] \right\} \tag{14}$$

The equation is unchanged if K_p, A_{i1}, and A_{i2} each have the same sign. Because minor H_4 is the critical term in stability determination for both the first and third quadrants, the stable regions in each of these quadrants are of the same area (fig. 4).

The comfortable region (fig. 5) is defined by the estimated region of comfortable control as derived from the previously developed restrained pilot parameters. The comfortable region is located near the origin and quite close to the approximate stability limit, rather than in the center of the stable area. An increase in the damping constant appears to be all that is necessary to vary the A_{i2} parameter values from the stability borderline to the comfortable region. Although the magnitude of this increase varies from case to case, preliminary investigations indicate it to be large.

A qualitative analysis of the interaction between the system-damping coefficient and the spring constant (fig. 9) reveals that, as the system masses and inertias are increased, larger values of the damping coefficient and spring constant are necessary to maintain system characteristics corresponding to a specific point in the A_{ij} plane.

Stable-Area Dependence Upon Pilot-Describing Parameters

The complexity of definition involved in vehicle-describing terms A_{ij} necessitates that only general observations be made concerning the dependence of stability maps upon pilot-describing parameters. The first of these parameters, pilot gain K_p inversely affects the stable region. As predicted by theory, an increase in the absolute value of the gain reduces the stable area. In a similar manner, an increase of the lag-time constant T_I also increases the area within the stable border. The largest stable areas are approached as the lag-time constant approaches its upper limit of 25. An increase in the lead time T_L tends to move the stable area toward the A_{i1} axis, thus reducing the range of A_{i2} values.

Nyquist Plots

Redefinition of stability criteria in terms of Nyquist plots provides a means of verifying results obtained by previous methods. Such a verification reveals the system to be conditionally stable; the gain can be increased or decreased to yield system instability. In accord with the previously established pilot-parameter range, the maximum gain allowing system stability is approximately 5 (fig. 6).

The previously discussed extension of the Nyquist procedure (eq. (17)) provides a means of expressing the ratio of output to input M as a function of the A_{ij} vehicle parameters. Such an expression is presented in figure 7 for the pilot-preferred simple gain situation. A ratio of output to input in excess of 4 corresponds to the Hurwitz criterion A_{ij} vehicle-parameter stability borderline. Figure 8 is an extension and simplification of the correspondence between the stability limits determined by the ratio of output to input M and the stability limits determined by the Hurwitz criterion. Since acceptable stability requires that $1 < M \leq 1.4$ (ref. 2), the vehicle parameter-established stable region contains only a small region in which acceptable stability is actually obtained. In the remaining area, the transient oscillatory response in the ratio of output to input is too extreme to be desirable. Thus, the majority of the area within the Hurwitz stability map has a very small degree of stability.

CONCLUSIONS

Tentative conclusions, which are pertinent as parameters in the design of a lunar flying vehicle, can be drawn from this work.

1. Vehicle-describing parameters A_{i1} and A_{i2} should have the same sign. For this reason, stable regions of equal area exist in quadrants one and three of the A_{i1}-A_{i2} plane (fig. 4).

2. The stable region is large to the extent that few restraints can be placed on vehicle characteristics without a knowledge of the system spring and damping constants.

3. The degree of stability in much of the stable region is very small (fig. 8).

4. A stable region exists where the pilot can act as a simple gain.

5. The estimated region of comfortable control within the stability map is located close to both the origin and the stability limit (fig. 5).

6. The area of acceptable system response (fig. 8) indicates that a small value of the A_{i1} vehicle parameter is preferable. Because an increase in inertia of the controlled element decreases the value of A_{i1}, large values of inertia are not necessarily detrimental. Of primary importance, however, is the relationship between inertia and the other system parameters (mass, thrust, length).

7. Stabilization of an unfavorable thrust-vector vehicle configuration requires smaller values of the system spring and damping constants than does stabilization of an unfavorable kinesthetic vehicle configuration.

8. A kinesthetically controlled vehicle configuration allows less freedom in vehicle-design definition because the physical pilot parameters (mass, length, inertia) cannot be adjusted to meet stability criteria.

9. Certain favorable vehicle configurations present themselves (fig. 11).

REFERENCES

1. Hall, David L.: A Mathematical Analysis of the Stability of a Lunar Flying Vehicle with Manual Controls. NASA General Working Paper No. 10,079, 1968.

2. D'Azzo, John J.; and Houpis, Constantine H.: Feedback Control System Analysis and Synthesis. McGraw-Hill Book Co., Inc., New York, 1966.

3. Skolnik, Alfred: Stability and Performance of Manned Control Systems. IEEE Transactions on Human Factors in Electronics, Vol. HFE-7, No. 3, 1966, pp. 115-124.

4. McRuer, Duane; Graham, Dunstan; Krendel, Ezra; and Reisener, Jr., William: Human Pilot Dynamics in Compensatory Systems. Air Force Flight Dynamics Laboratory, Technical Report No. AFFDLTR-65-15, July 1965.

BIBLIOGRAPHY

Del Toro, Vincent; and Parker, Sydney R.: Principles of Control System Engineering. McGraw-Hill Book Co., Inc., New York, 1960.

Etkin, Bernard: Dynamics of Flight, Stability, and Control. John Wiley and Sons, Inc., New York, 1959.

Jex, H. R.; McDonnell, J. D.; and Phatak, A. V.: A Critical Tracking Task for Manual Control Research. IEEE Transactions on Human Factors in Electronics, Vol. HFE-7, No. 4, 1966, pp. 138-145.

Summers, L. G.; and Ziedman, K.: A Study of Control Methodology with Annotated Bibliography. NASA CR-125, 1964.

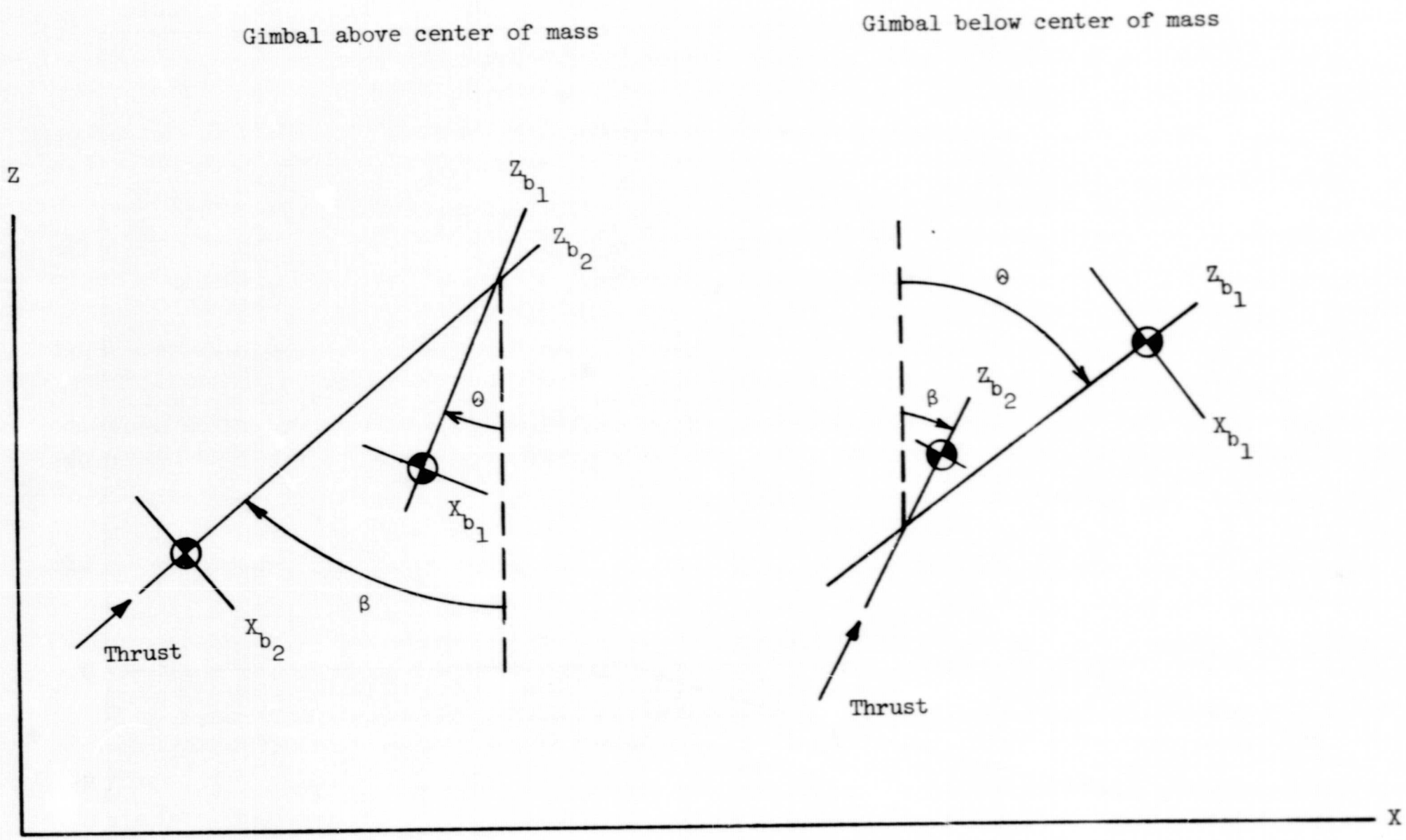

Figure 1.- Vehicle coordinate system for kinesthetic- and thrust-vector control.

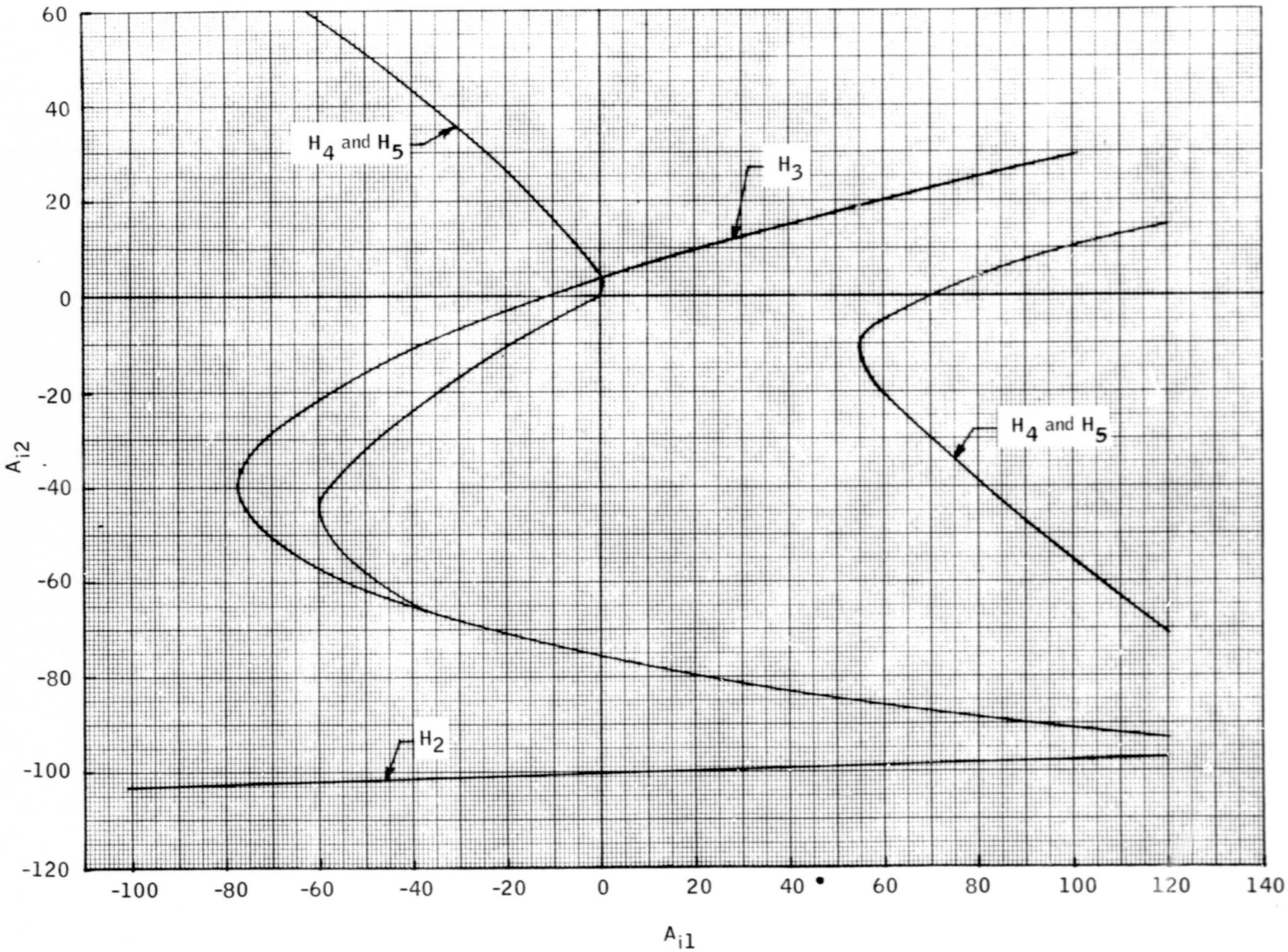

Figure 2.- Hurwitz-minor zero lines.

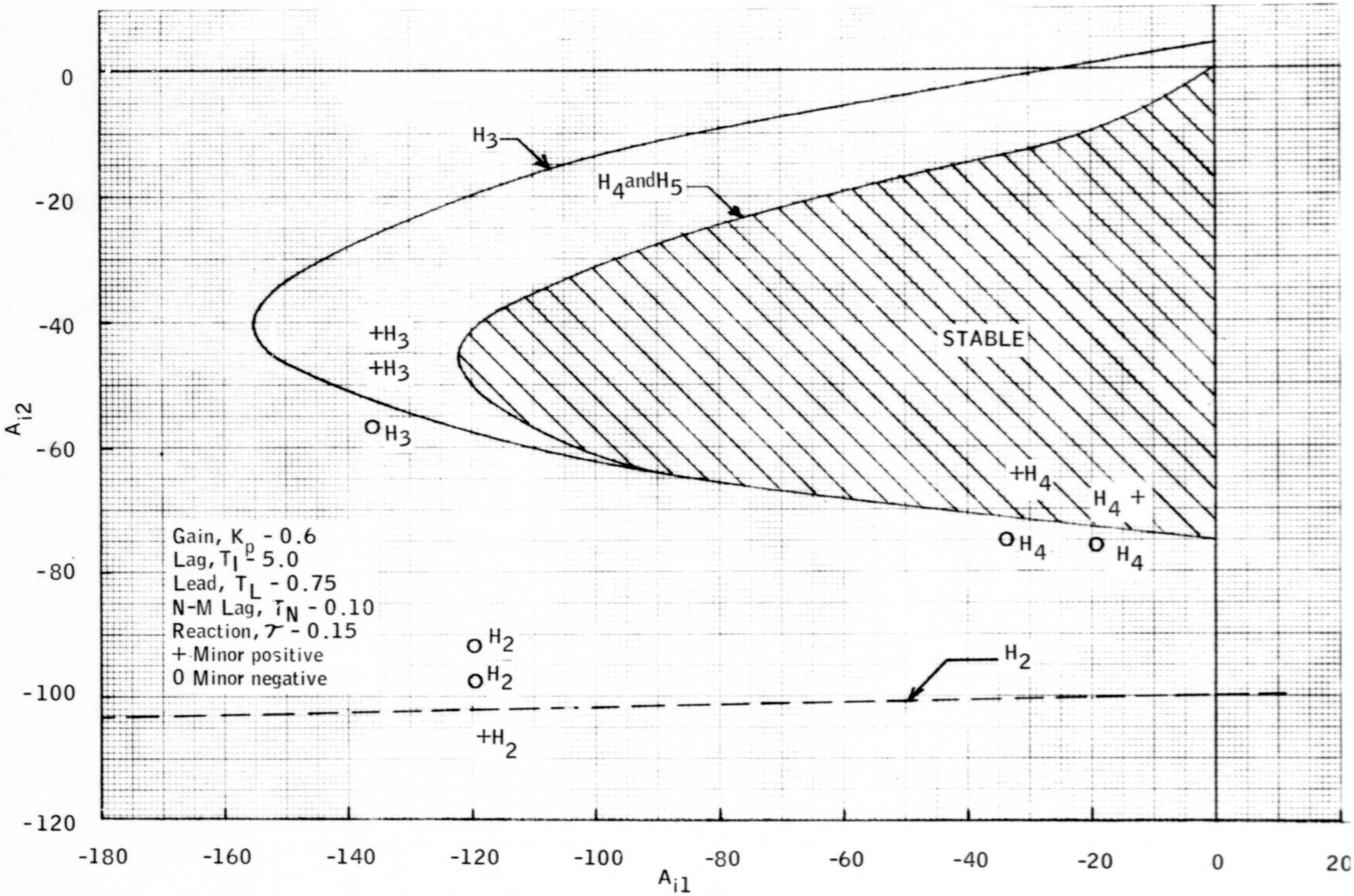

Figure 3.- Stability interpretation of Hurwitz-minor zero lines.

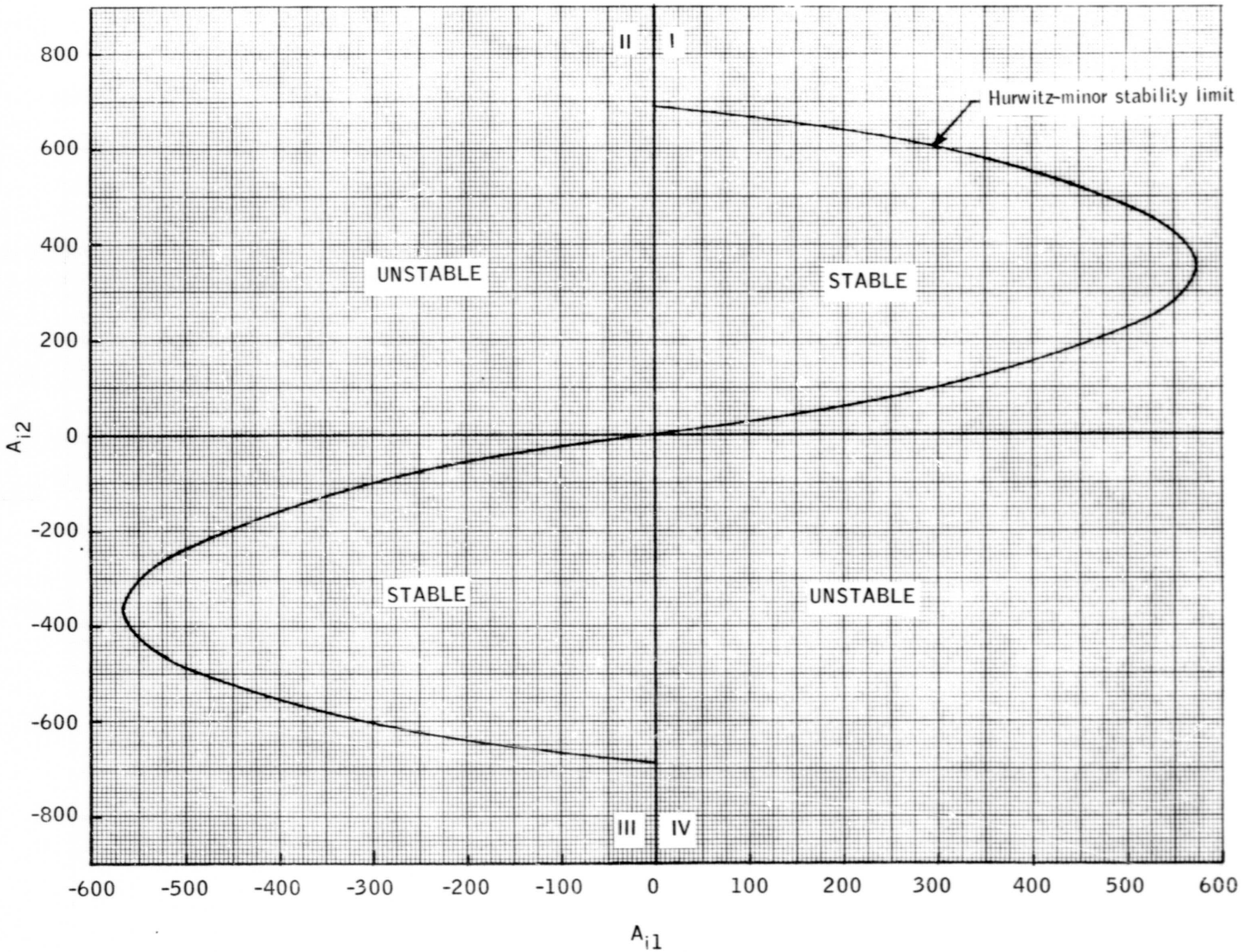

Figure 4.- Stable-region definition in the A_{i1}-A_{i2} plane.

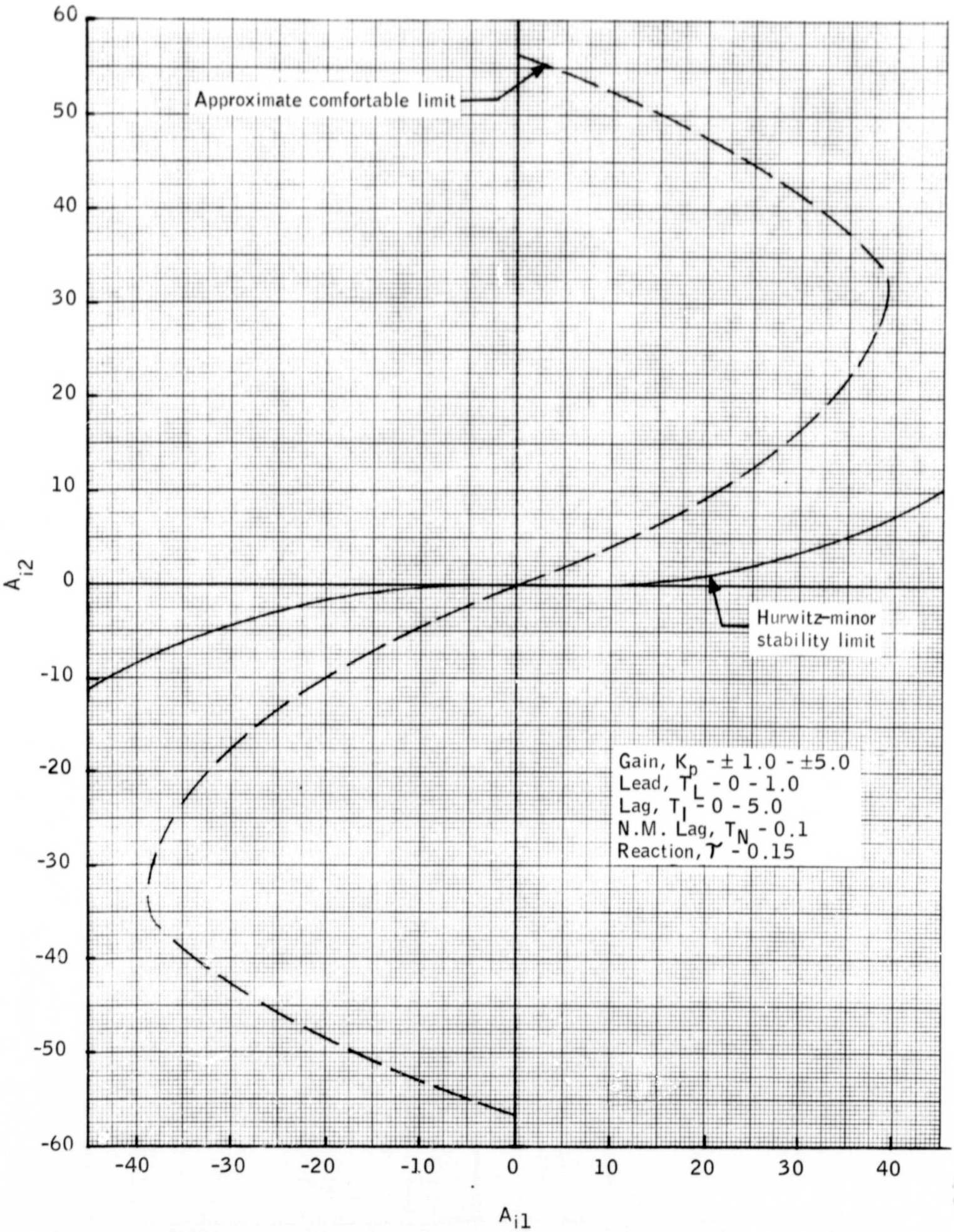

Figure 5.- Stability limit for comfortable human-parameter values in the A_{i1}-A_{i2} plane.

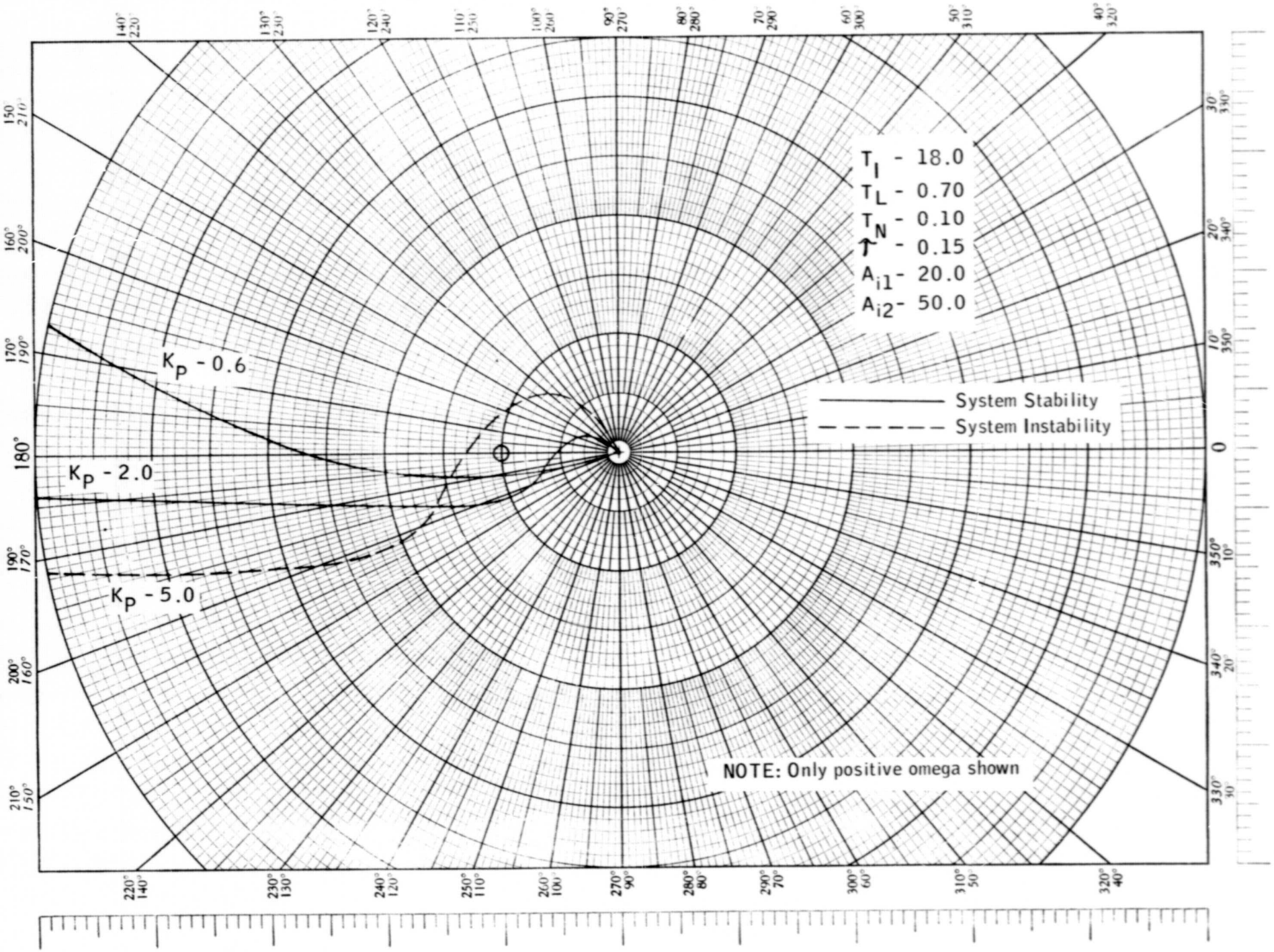

Figure 6. - System-stability dependence upon pilot gain as exhibited by Nyquist plots.

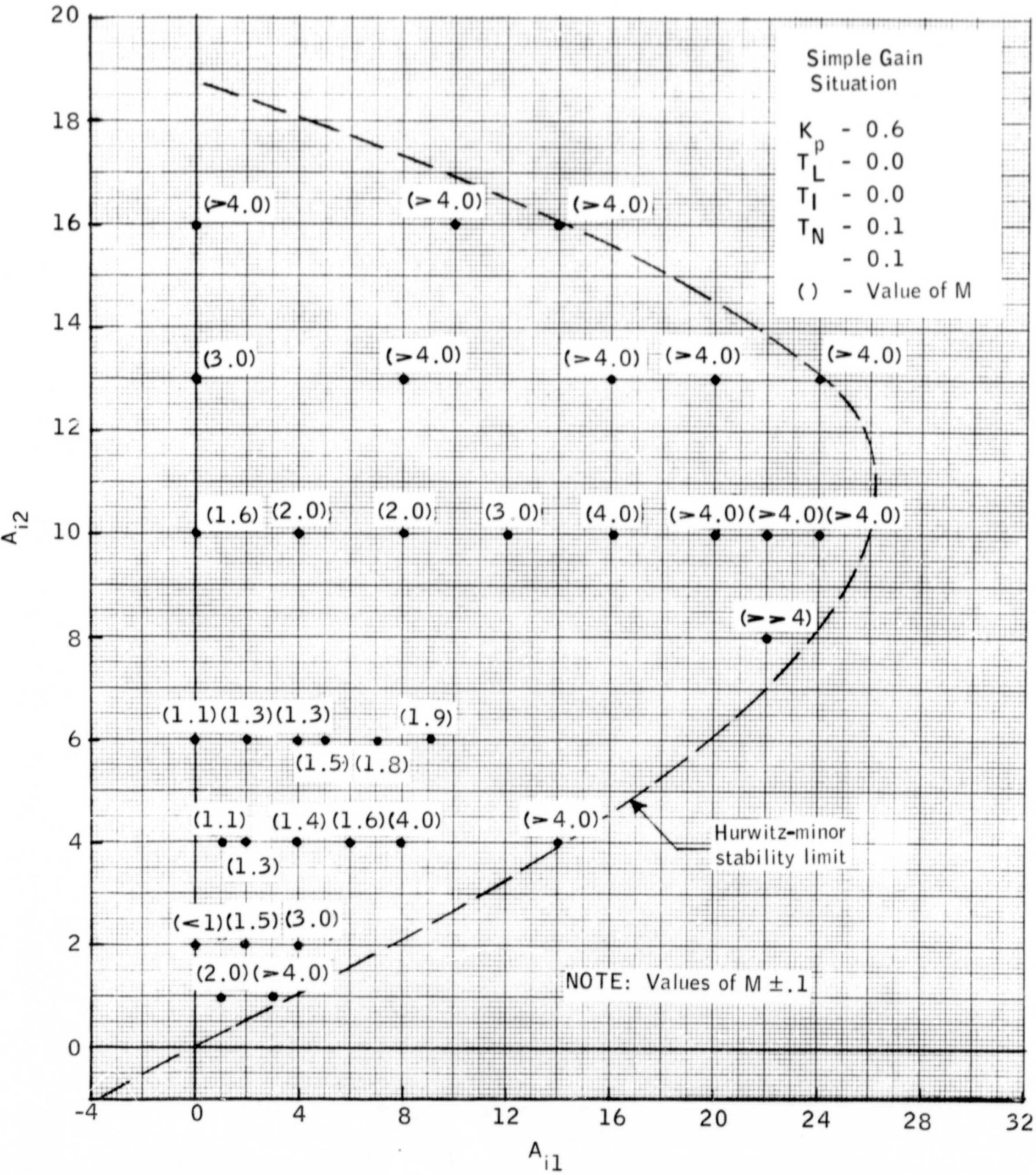

Figure 7.- Ratio M of output to input as a function of vehicle parameters A_{i1} and A_{i2}.

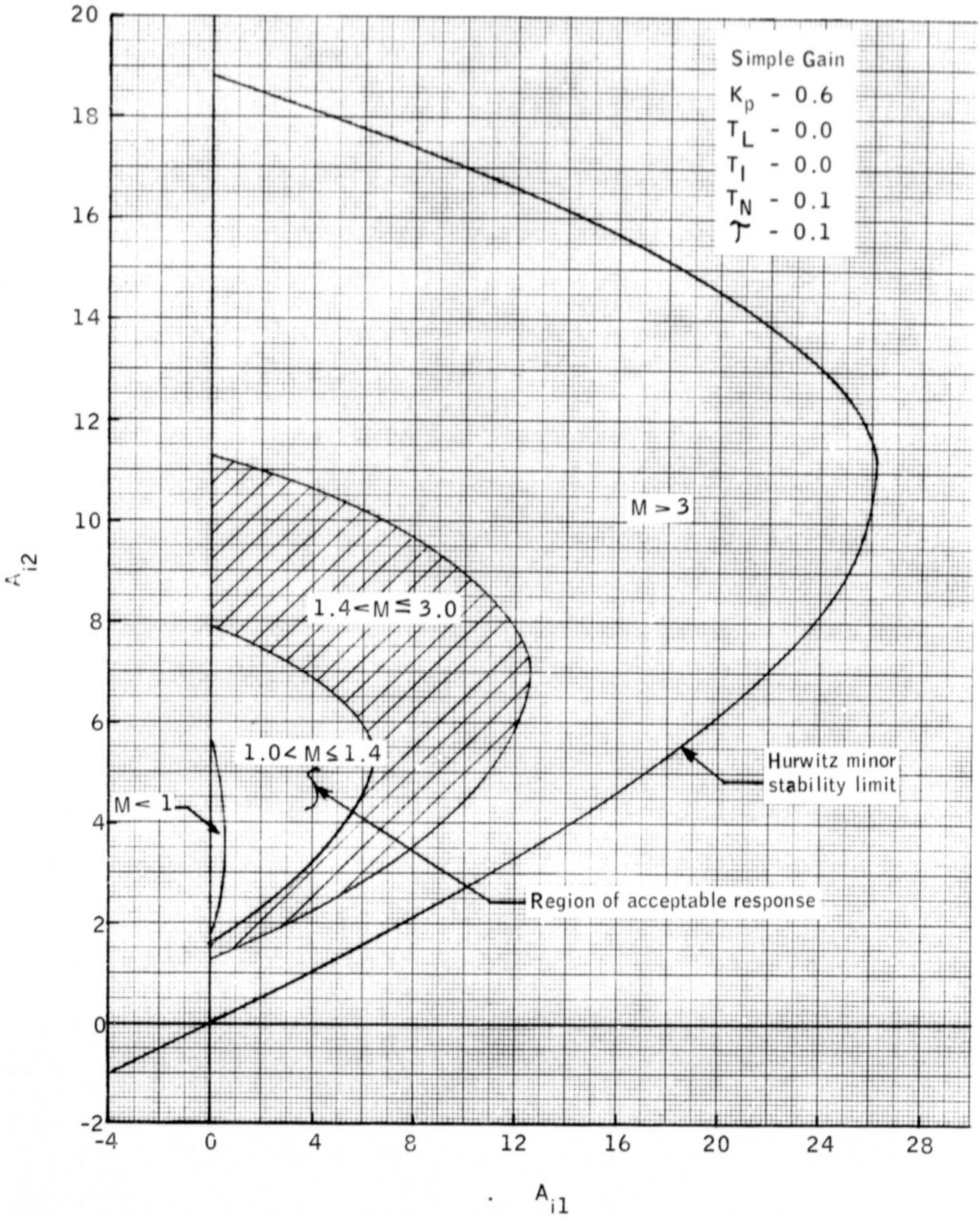

Figure 8.- Comparison of A_{i1}-A_{i2} stable regions as determined by the ratio M of output to input and the Hurwitz-minor zero line.

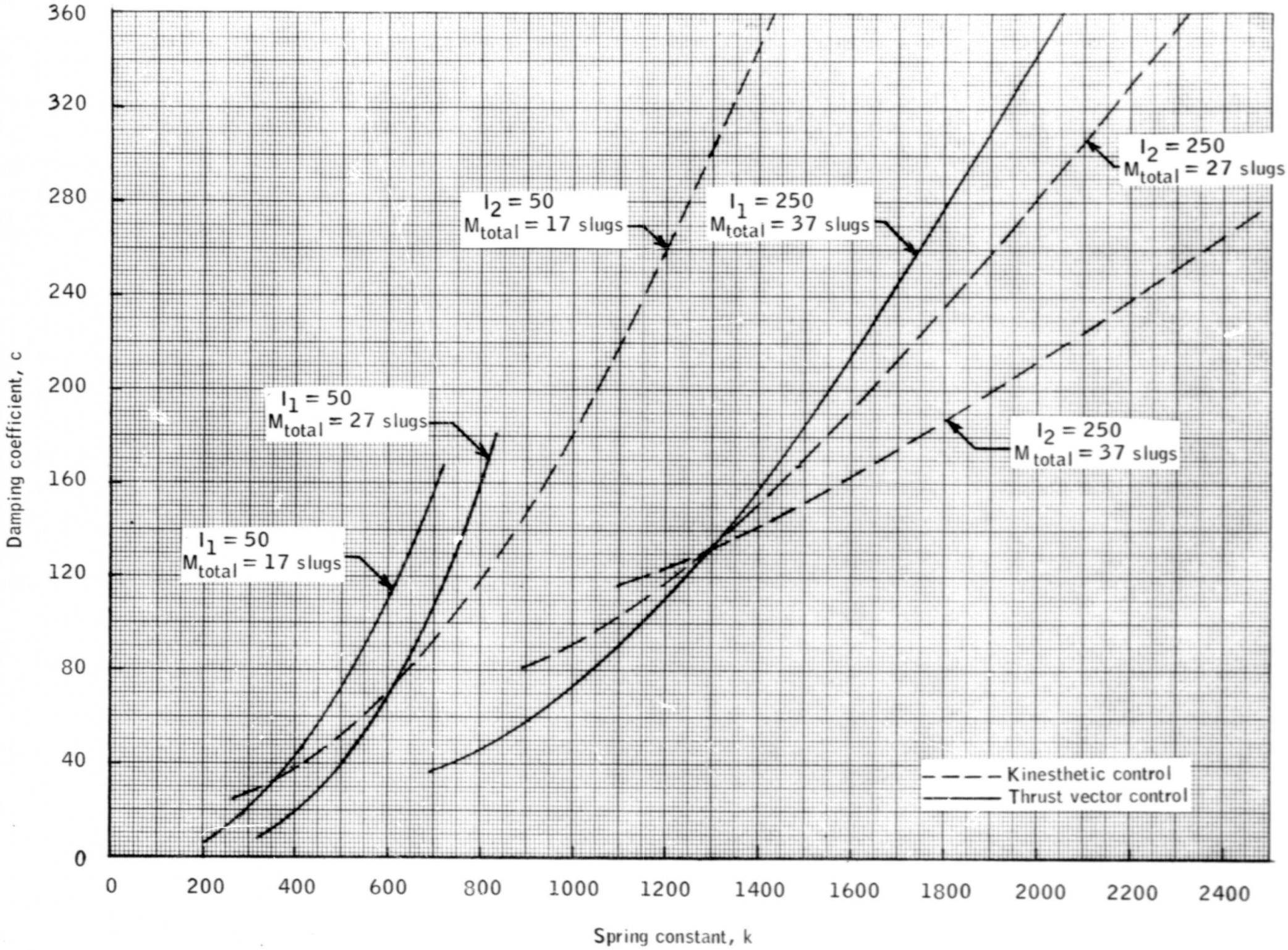

Figure 9.- Spring constant as a function of damping coefficient for various stable vehicle configurations.

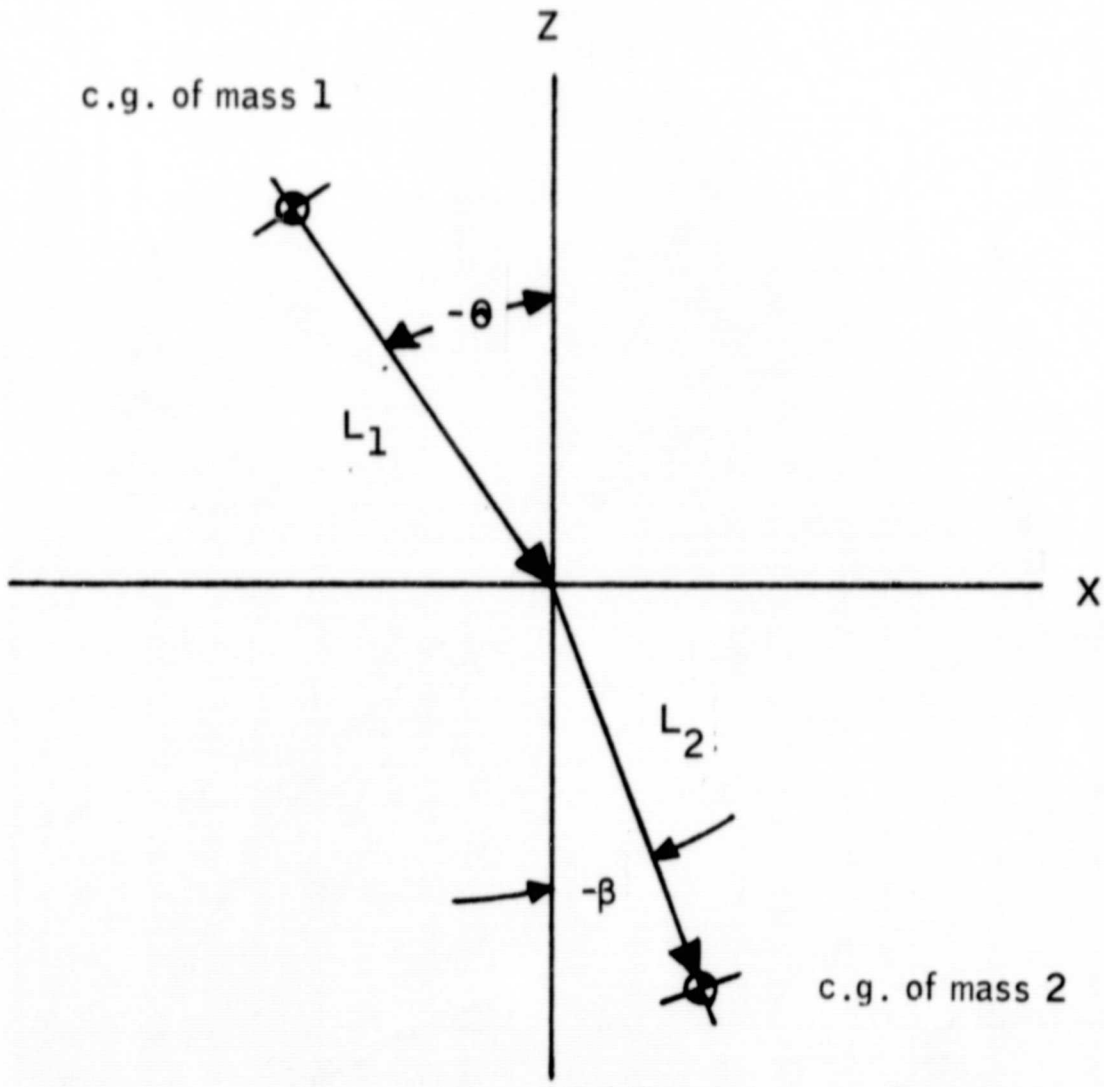

Figure 10.- Vehicle configuration with one mass above and the other mass below the gimbal point.

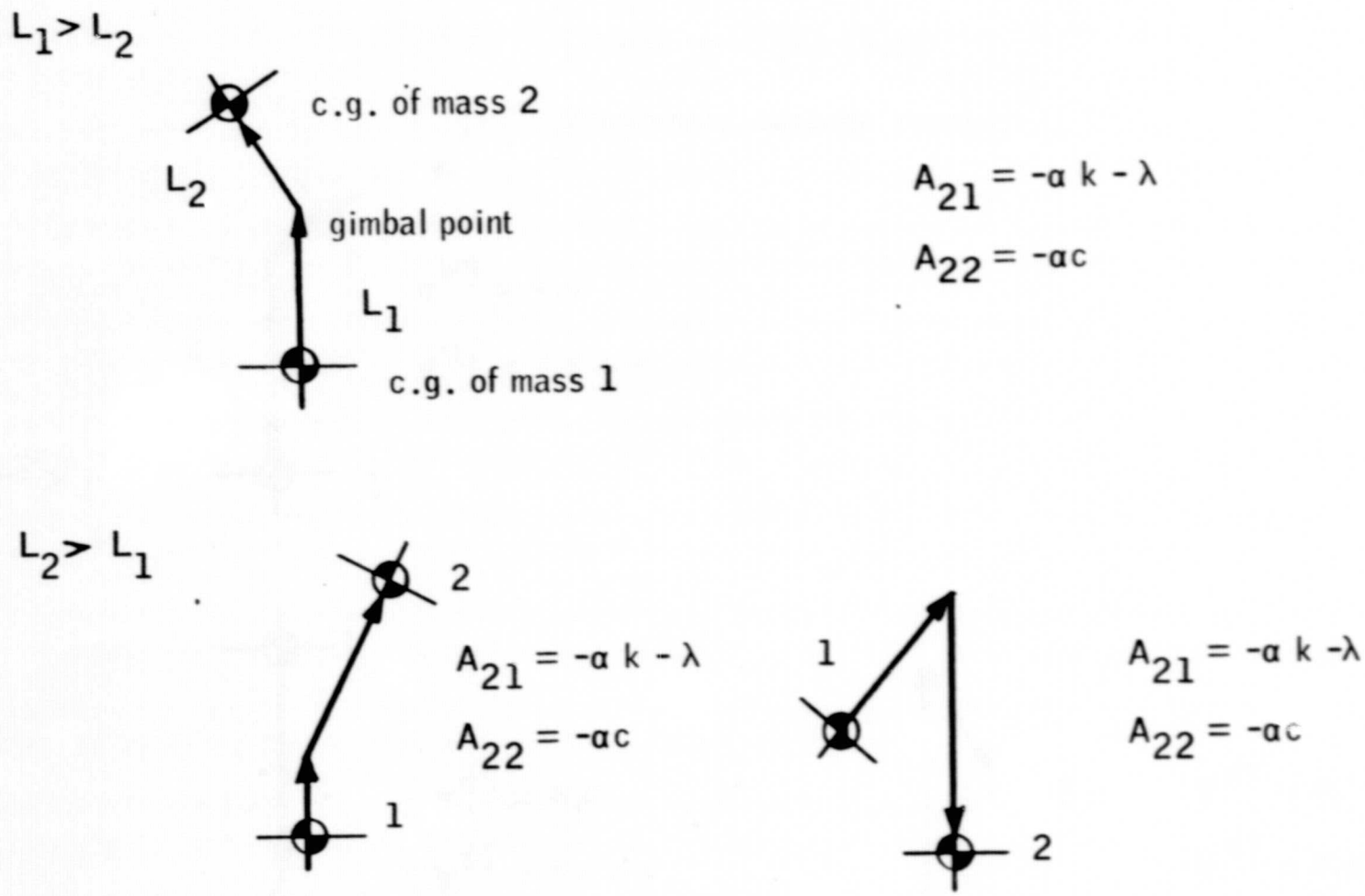

(a) Thrust-vector control.

Figure 11.- Favorable vehicle configurations.

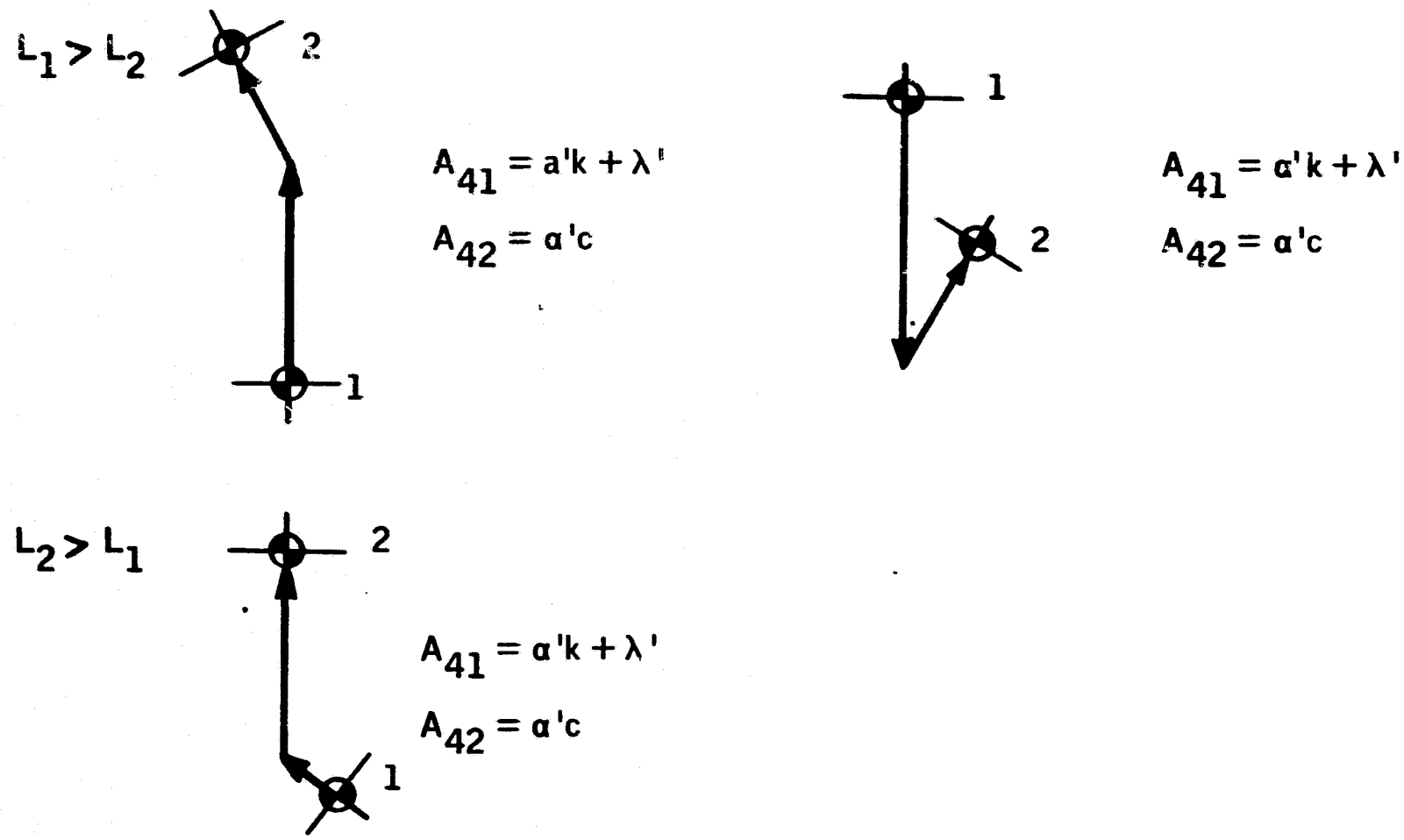

(b) Kinesthetic vehicle control.

Figure 11.- Concluded.